AIP | Journal of Applied Physics

# Field-emission-assisted approach to dry micro-electro-discharge machining of carbon-nanotube forests

Tanveer Saleh, Masoud Dahmardeh, Anas Bsoul, Alireza Nojeh, and Kenichi Takahata

Citation: J. Appl. Phys. **110**, 103305 (2011); doi: 10.1063/1.3663438
View online: http://dx.doi.org/10.1063/1.3663438
View Table of Contents: http://jap.aip.org/resource/1/JAPIAU/v110/i10
Published by the American Institute of Physics.

# Field-emission-assisted approach to dry micro-electro-discharge machining of carbon-nanotube forests

Tanveer Saleh,[1,2] Masoud Dahmardeh,[1] Anas Bsoul,[1,3] Alireza Nojeh,[1,a)] and Kenichi Takahata[1,a)]
[1]*Department of Electrical and Computer Engineering, University of British Columbia, Vancouver, BC V6T 1Z4, Canada*
[2]*FARCAMT, Industrial Engineering Department, College of Engineering, King Saud University, Riyadh 11421, Saudi Arabia*
[3]*Department of Computer Engineering, Jordan University of Science and Technology, Irbid, Jordan*

(Received 10 July 2011; accepted 27 October 2011; published online 29 November 2011)

This work investigates dry micro-electro-discharge machining ($\mu$EDM) of vertically aligned carbon nanotube (CNT) forests that are used as cathodes in the process, as opposed to conventional $\mu$EDM where the material to be machined forms the anode, toward achieving higher precision in the patterned microstructures. The new configuration with the reversed polarity is observed to generate higher discharge currents in the process, presumably due to effective field-emission from CNTs. This effect allows the process to be performed at very low discharge energies, approximately 80× smaller than in the conventional normal-polarity case, with the machining voltage and tolerance down to 10 V and 2.5 $\mu$m, respectively, enabling high-precision high-aspect-ratio micropatterning in the forests. The new approach is also demonstrated to make the process faster, cleaner, and more stable than conventional processing. Spectroscopic analyses of the forests processed by reverse $\mu$EDM show no evidence of significant crystalline deterioration or contamination in the CNTs. © *2011 American Institute of Physics*. [doi:10.1063/1.3663438]

## I. INTRODUCTION

Carbon nanotubes (CNTs) have highly attractive mechanical, electrical, optical, and thermal properties.[1–5] Densely packed, vertically aligned CNTs are commonly referred to as CNT forests and have many potential engineering applications in the field of micro-electro-mechanical systems (MEMS),[6] micro-chip heat sinks,[7] field-emitters,[8–10] gas sensors,[11] photovoltaics,[12] fuel cells,[13] and synthetic unidirectional adhesive tapes.[14] It is very important to pattern CNT forests to make them useful for many of the above applications. The formation of patterned CNT forests has widely been conducted through selective growth of the forests by chemical vapor deposition (CVD) on pre-patterned catalyst on the substrate. However, this technique is limited to producing two-dimensional patterns with uniform height. Micropatterning of three-dimensional, free-form structures with high aspect ratios in pure CNT forests was recently demonstrated using a process based on micro-electro-discharge machining ($\mu$EDM).[15,16] Dry air was used as the dielectric medium in the process, instead of the dielectric liquid used in typical $\mu$EDM, as the forest structures patterned in liquid are drastically modified when the structures are dried because of the capillary effect.[15] The optimal machining condition was observed at the discharge voltage of 30 V. This technique was further investigated in Refs. 16 and 17. These studies revealed a possible removal mechanism of CNT forests in dry $\mu$EDM, suggesting that the process is essentially oxygen plasma etching rather than the conventional, direct thermal removal (evaporation and melting) process. The role of oxygen in the process was also investigated and it was reported that air was an optimal medium for $\mu$EDM of CNT forests. The EDM condition at 60 V and 10 pF was effective in creating needle-like microstructure arrays in CNT forests.[16] The machining tolerance, or the discharge gap clearance between a forest and the $\mu$EDM electrode, was reported to be 10 $\mu$m or more, substantially larger than typical values (of one to a few micrometers) involved in standard $\mu$EDM with dielectric liquid. Toward achieving higher precision and nano-scale removal in dry $\mu$EDM of CNT forests, it is essential to minimize the discharge voltage and the discharge gap while achieving effective removal of CNTs.

In typical EDM (including $\mu$EDM), the workpiece and the electrode are generally arranged to be the anode and the cathode, respectively, as this polarity usually results in efficient material removal with small electrode wear. To the best of the authors' knowledge, all previous studies on carbon-nanofiber or CNT-forest $\mu$EDM have used this conventional polarity, i.e., the carbon material has served as the anode while the tungsten electrode has been used as the cathode.[15–17] However, the effect of the polarity of the CNT forest on the EDM removal of the material has not been studied. Because of their extremely small tips with nanometer radii and high aspect ratios, CNTs are known to significantly enhance an applied electric field and thus have excellent electron emission properties. In fact, CNT cathodes were reported to reduce gas breakdown voltage while increasing the discharge current compared to tungsten cathodes;[18] although the set-up and the ranges of the breakdown voltage

a)Authors to whom correspondence should be addressed. Electronic mail: anojeh@ece.ubc.ca and takahata@ece.ubc.ca.

 

and current reported are different (one to two orders of magnitude) from those involved in $\mu$EDM, the above suggests that the use of reverse polarity in $\mu$EDM of CNT forests could be effective in lowering the discharge voltage and gap clearance (for higher precision) as well as increasing the discharge current (for effective CNT removal) in the process. To explore this hypothesis, the present work investigates reverse-polarity $\mu$EDM of pure CNT forests in dry air experimentally. The characteristics of reverse $\mu$EDM for CNT forests and the patterned structures are studied to reveal various advantages over the conventional process with the normal polarity, achieving higher precision in the forest patterning process including that for high-aspect-ratio geometries.

## II. EXPERIMENTAL SET-UP

The CNT forest samples used in this study were grown on highly doped silicon substrates ($\langle 100 \rangle$ n-type, resistivity 0.008-0.015 $\Omega$·cm) using an atmospheric-pressure CVD system. The samples were prepared as follows: First, a 10-nm-thick layer of aluminum was evaporated on the silicon wafer. Subsequently, a 1-nm-thick layer of iron was deposited. The CNT growth was performed by placing the sample on a piece of a lightly doped Si wafer that served as the resistive heater (CNT growth zone) in the reaction tube of the system. A pre-heater was used to heat up the gas at ~30 cm before reaching the growth zone. In a typical growth process, after loading the sample, the pre-heater's temperature was ramped up from room temperature to 850 °C in 20 min while maintaining a flow of 400 sccm of argon. Then the silicon heater was turned on to maintain the temperature of the sample at ~750 °C for 2 min. The sample was annealed for 5 min under 140 sccm of argon and 400 sccm of hydrogen. Subsequently, flow rates of 140 sccm of ethylene, 400 sccm of hydrogen, and 100 sccm of argon were used for 15 min for the CNT growth. The growth was ended by turning off the silicon heater and all the gas flows except for 400 sccm of argon for about 20 min to cool the pre-heater down to room temperature. This process yielded forests of vertically aligned multi-walled CNTs with lengths of up to several 100's of $\mu$m.

The experiments for $\mu$EDM of the CNT forests were performed using a servo-controlled 3-axis $\mu$EDM system (EM203, SmalTec International, IL, USA) with a 0.1-$\mu$m positioning resolution. The discharge pulses were generated with a relaxation-type resistor-capacitor (*R-C*) circuit,[19] a proven pulse generator used for $\mu$EDM of CNTs.[15–17] The experimental set-up arranged for the machining tests and characterization is illustrated in Fig. 1. As shown, a current probe (CT-1, Tektronix, USA) was used to monitor pulses of the discharge current in real time. The discharge current data were captured from the oscilloscope using a GPIB interface and stored in a computer for subsequent analysis. A series of $\mu$EDM experiments at both normal and reverse polarities were performed for various energy levels that were controlled by varying the discharge voltage in a range of 10-60 V with a fixed capacitance of 10 pF in the *R-C* circuit. The electrode (tungsten, diameter of 40-93 $\mu$m) was rotated at 3000 rpm during all the machining experiments. The X-Y scanning rate and the electrode feed rate in the Z direction were set to 1 mm/min and 10 $\mu$m/min, respectively.

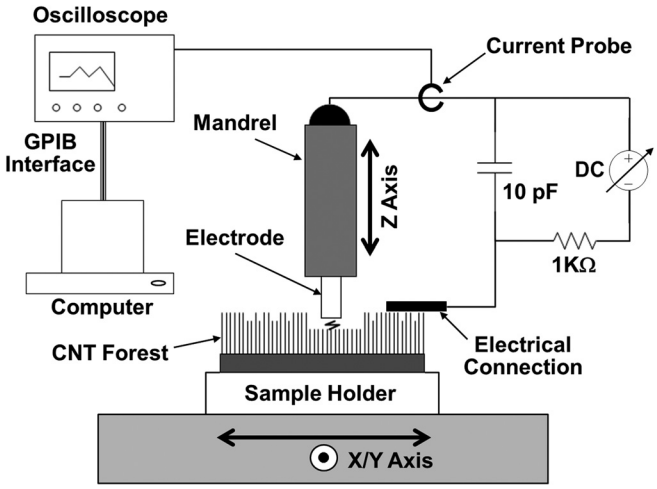


FIG. 1. The experimental set-up used for characterization of reverse-polarity $\mu$EDM of CNT forests.

## III. RESULTS AND DISCUSSION

The discharge pulses generated with both reverse and normal polarities were first characterized to observe the differences between the two conditions. Figures 2(a) and 2(b) show the comparison of the average peak current and frequency of the pulses (n = 400) measured at different voltage levels. Typical discharge pulses for the normal and reverse polarities measured with the current probe are also shown in Figs. 2(c) and 2(d). It can be understood from the comparison in Figs. 2(a) and 2(b) that both the peak current and the frequency with the reverse polarity are higher than those with the normal polarity, and that the difference in the peak current at lower voltages is significant. It was also observed that short circuiting between the electrode and the CNT forest was a predominant factor in the normal polarity case when lower voltages were used (e.g., for 10 V and 10 pF, the probability of short circuits with the normal polarity was ~5× higher than that with the reverse polarity). More occurrences of short circuits may result in mechanical grinding of the CNT forest as observed in Ref. 15, which can distort the orientation of the CNTs. A possible reason behind the higher discharge current in the reverse-polarity case that uses the forest as the cathode could be enhanced field-emission (FE) from CNTs;[10,20–23] the forest cathode can more easily emit electrons from the nano-scale tips of the CNTs compared to a conventional metallic cathode (such as the tungsten tip) at a given voltage. The increased discharge current with the reverse polarity is also consistent with the results reported in Ref. 18.

As will be discussed later, the reverse-polarity condition at 10 V was found to produce an approximate discharge gap clearance of 2.5 $\mu$m; this means that the applied electric field established at the gap is ~4 V/$\mu$m under the condition. Past studies show FE current densities of ~0.5 mA/cm$^2$ for tungsten cathodes[24] and ~1 mA/cm$^2$ for CNT-forest cathodes[10] for this level of field, suggesting an approximately 2× increase in the FE current with the CNT forest compared to

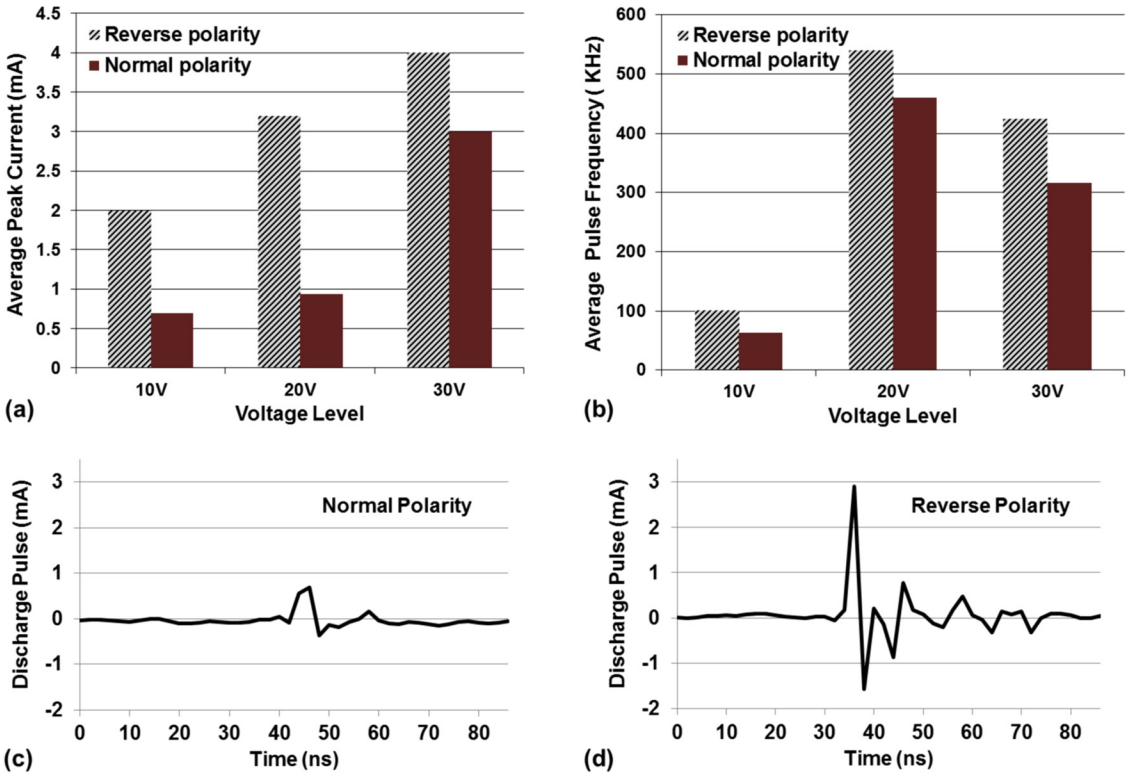


FIG. 2. (Color online) (a) Average peak current of discharge pulses measured at different voltages (with constant capacitance of 10 pF), (b) average pulse frequency at the same voltages and capacitance, and typical single pulse of discharge current generated using 20 V and 10 pF with (c) normal polarity and (d) reverse polarity. A tungsten electrode with a 93-$\mu$m diameter was used for all the measurements.

tungsten. Another study shows that discharge currents (in a corona phase) with CNT-forest cathodes are 6-7× larger than those with tungsten cathodes.[18] The discharge current densities calculated from Fig. 2(a) at 10 V for the normal and reverse polarities (assuming that the current is uniformly distributed over the bottom surface of the 93-$\mu$m-diameter electrode) are 10.3 A/cm$^2$ and 29.5 A/cm$^2$, respectively, giving a 2.86× increase in the discharge current when the reverse polarity or the CNT-forest cathode is used. It is notable that although the discharge conditions and properties involved in the above cases (FE, corona, and arc) are substantially different,[25] the levels of current enhancement observed with CNT-forest cathodes are somewhat similar under the experimental conditions used.

It should also be noted that at high discharge voltages (>50 V), the pulse frequency was not necessarily higher for the reverse polarity, contrary to what was observed for low voltages as shown in Fig. 2(b). At 60 V and 10 pF, for example, the pulse frequency with the reverse polarity was measured to be ~90 KHz, whereas that with the normal polarity was ~1360 KHz. This is likely related to the fact that the operation at high voltages with the reverse polarity often produced uncontrolled large sparks, which resulted in an abnormally large removal of the forest material and a very large gap clearance between the electrode and the forest, preventing discharge generation until the gap was reduced by the electrode feeding motion. This problematic phenomenon caused not only the decrease of the pulse frequency but also damages to the forest structure. In contrast, normal-polarity machining at high voltages was observed to produce stable discharge pulses with nearly no short circuiting, leading to higher frequency. This process dependence on the voltage polarity at high voltages can be clearly seen in the results shown in Fig. 3 that compares square patterns produced under identical voltage and capacitance (60 V and 10 pF) with normal and reverse polarities. The significant distortion of the pattern for the reverse-polarity case is evident. This result is most likely due to the occurrence of the uncontrolled large sparks under the high-voltage condition mentioned earlier; at voltages greater than 50 V, more effective and efficient removal was possible with the normal-polarity condition.

It was found that for lower voltages, however, the reverse-polarity $\mu$EDM exhibited a different behavior, with advantageous effects towards further miniaturization in the CNT removal process with higher precision. The previous studies reported that the lowest value of the optimal voltage with the normal polarity was around 30 V, and that further lowering of the voltage led to mechanical grinding of the CNTs.[15] To evaluate the effect of the reverse polarity in $\mu$EDM of the forest for comparison, first shallow cavities were machined on a CNT forest with both the polarities at low-voltage levels. As can be seen in the sample results at 20 V shown in Figs. 4(a) and 4(b), reverse-polarity machining produced smoother surfaces compared to normal-polarity processing. One possible cause of this result may be the difference in the discharge current between the two cases—the reverse-polarity process produces higher current than the normal-polarity for the same voltage as demonstrated in Fig. 2(a). This may allow the former to remove CNTs

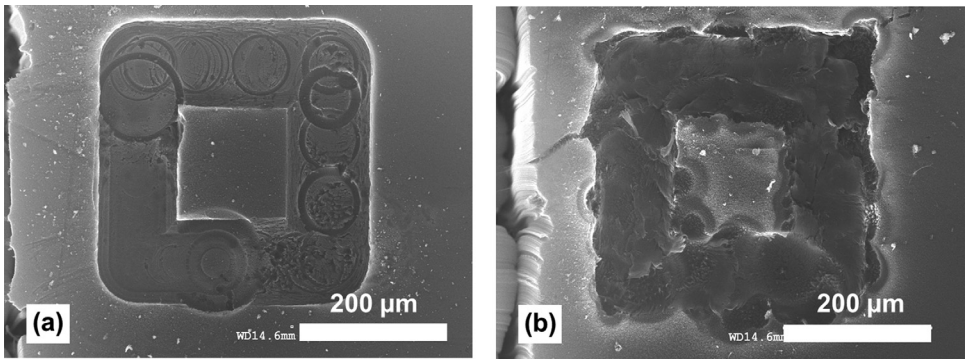


FIG. 3. Scanning electron microscope (SEM) images of micropatterns machined in a CNT forest using 60 V and 10 pF with (a) normal polarity and (b) reverse polarity. Each pattern was created by scanning a rotating electrode along a square shape (200 $\mu$m $\times$ 200 $\mu$m) in the X-Y plane with continuous feeding of the electrode in the Z direction.

effectively, whereas the latter suffers from insufficient removal because of smaller discharge currents, possibly causing mechanical abrasion of the forest. The above effect was further verified with deeper patterning with both polarities, in a similar manner as that described in Fig. 3 but at 10 V (with 10 pF) in this case. The results in Figs. 4(c) and 4(d) indicate that the reverse-polarity process produced sharper, smoother, and cleaner microstructures compared to the normal-polarity case. Moreover, the patterns created with the reverse polarity exhibited a narrower width in the machined grooves compared to those with the normal polarity even though identical electrode and machining conditions were used. From the dimensions shown in Fig. 4, as well as the diameter (93 $\mu$m) of the electrode used, the discharge gap clearance is calculated to be 7.5 $\mu$m for the normal polarity, whereas for the reverse polarity it is 2.5 $\mu$m, which is 3$\times$ smaller (and shows a $\sim$4$\times$ improvement over the previous result reported in Ref. 15). This means that reverse $\mu$EDM enables much tighter tolerances and higher precision in CNT forest patterning.

Machining stability is another important aspect of $\mu$EDM processing of CNT forests. In the process, electrode feeding is feedback controlled so that when a short circuit is detected, the Z stage retracts the electrode upward until the

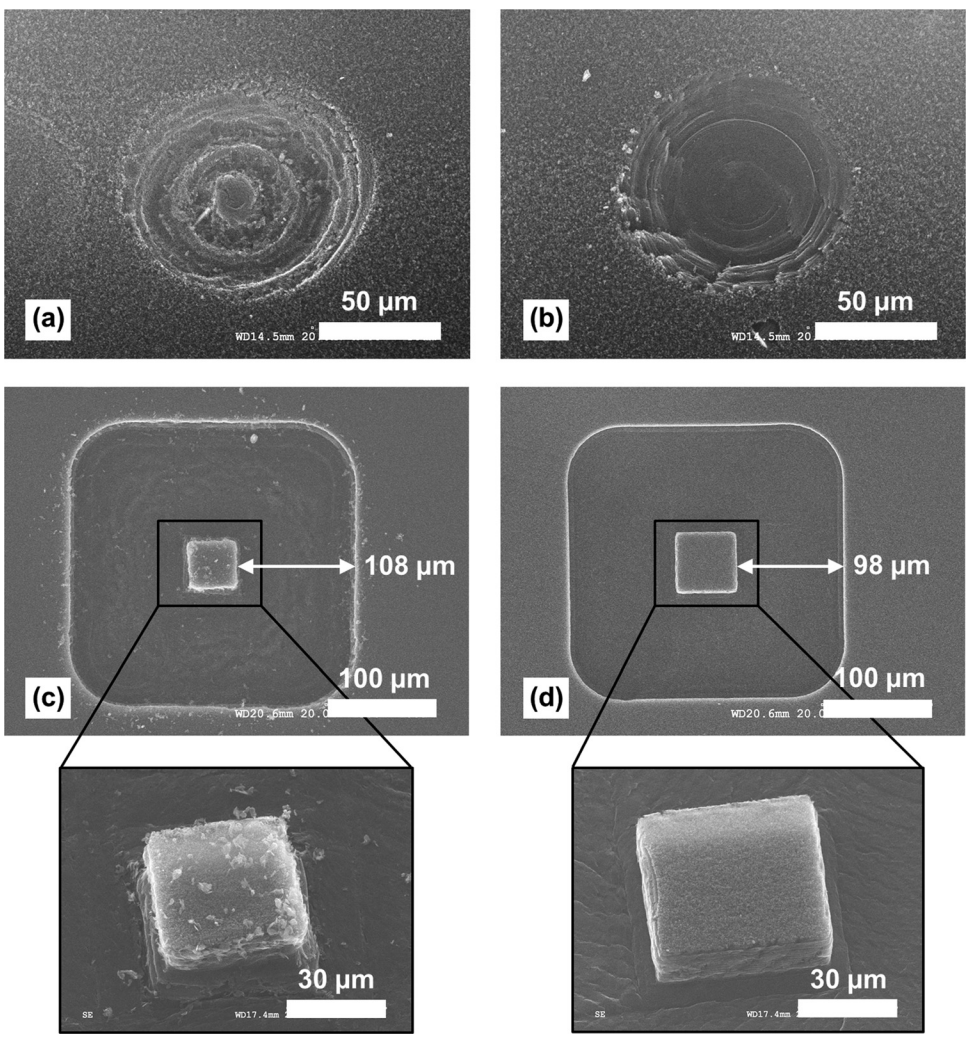


FIG. 4. The upper two SEM images show shallow cavities machined in a CNT forest using 20 V and 10 pF with (a) normal polarity and (b) reverse polarity. The lower two SEM images show micropatterns machined in a CNT forest using 10 V and 10 pF with (c) normal polarity and (d) reverse polarity, for a depth of 40 $\mu$m with 1-$\mu$m-step electrode feeding in the Z direction. The images in (c) and (d) also show close-up views of the microstructures created in the cavities.

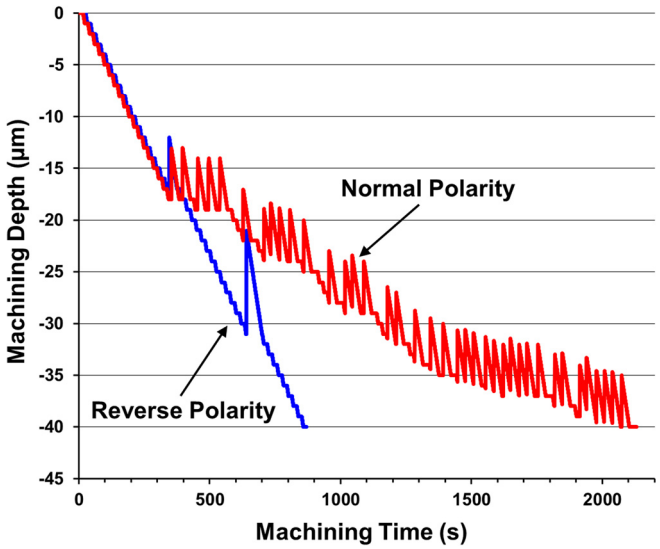


FIG. 5. (Color online) Electrode positions on the Z axis tracked in real time during machining with normal and reverse polarities, both using 10 V and 10 pF. In both cases, the electrode was scanned along a square shape (100 $\mu$m × 100 $\mu$m) in the X-Y plane with 1-$\mu$m-step feeding in the Z direction until reaching a depth of 40 $\mu$m.

circuit is opened and then moves the electrode downward to resume its feeding and the machining process. The process becomes unstable and slow if many short circuits occur during the process because of frequent up/down motion of the Z axis. It was observed that reverse-polarity machining at low voltages was consistently more stable than normal-polarity machining for CNT forests. This tendency can be seen in Fig. 5 that plots the electrode position on the Z axis during each of the machining processes conducted under the same conditions except for the voltage polarity. It is clear from the graph that the normal-polarity case produced frequent short circuits that led to ripples in the electrode motion, whereas the reverse-polarity case resulted in much more stable and faster electrode feeding or removal of the CNTs. For this particular machining condition, the total machining time with the reverse polarity was approximately 60% shorter than the time with the normal polarity.

Another interesting observation is that reverse-polarity machining (at low voltages) produced very small or almost no debris, leading to highly clean surfaces after the machining as can be seen in Fig. 4(d). In contrast, as reported in Ref. 15, normal-polarity machining produced a substantial amount of debris that was left on the machined surfaces [Fig. 4(c)]. It was also observed that the debris accumulated on and stuck to the electrode surfaces, increasing the effective diameter of the electrode in a random and non-uniform manner. In reverse $\mu$EDM, the forest is the cathode and thus not subject to electron bombardment (leading to the conventional thermal removal) in principle; therefore, CNT removal is expected to be almost entirely due to oxygen plasma etching that can decompose CNTs into volatile products, forming virtually no debris. With the normal-polarity condition, in contrast, the forest is the anode that is bombarded by electrons during the process and may be subject to some level of thermal removal where parts of the CNTs are melted and blown by pressure waves induced by the intense heat that the pulsed discharge arc produces, leaving resolidified carbon debris on the workzone and the electrode. A single MWCNT was reported to be heated up to 2000 K due to emitting a FE current of 1 $\mu$A;[26] this self-heating effect of CNTs may need to be considered with respect to the removal process. However, in the present case, the current passed through a single CNT by a discharge pulse is estimated to be significantly lower, e.g., ~300 pA for the 10 V condition that involves an average peak discharge current of 2 mA [Fig. 2(a)] considering the typical CNT density of $\sim 10^{11}/\text{cm}^2$ observed in the forest samples and the electrode diameter of 93 $\mu$m used in the experiment. Moreover, the $\mu$EDM process uses pulsed currents as opposed to DC current involved in Ref. 26. Therefore, the impact of the self-heating effect on the removal process is likley minimal under the relevant machining condition.

A key factor for high-aspect-ratio patterning in CNT forets is debris removal.[15] It is also essential to maintain the electrode surfaces free from debris accumulation that degrades the machining precision and can destroy the high-aspect-ratio microstructures produced during the process. It was observed in the present study that the use of a relatively high discharge energy (e.g., 60 V and 10 pF) was effective in reducing debris generation under the normal polarity condition (in Ref. 16, needle-like microstructures were created with this method), which could be due to the enhancement of the oxygen-plasma etching phenomenon; however, the use of higher voltages tends to cause lower tolerance and more roughness in the machined surfaces. All these issues may be effectively addressed through reverse $\mu$EDM because of its cleanness and the possibililty of usage of low voltages as discussed above. The effectiveness of reverse $\mu$EDM in high-aspect-ratio micromachining of CNT forests was evaluated

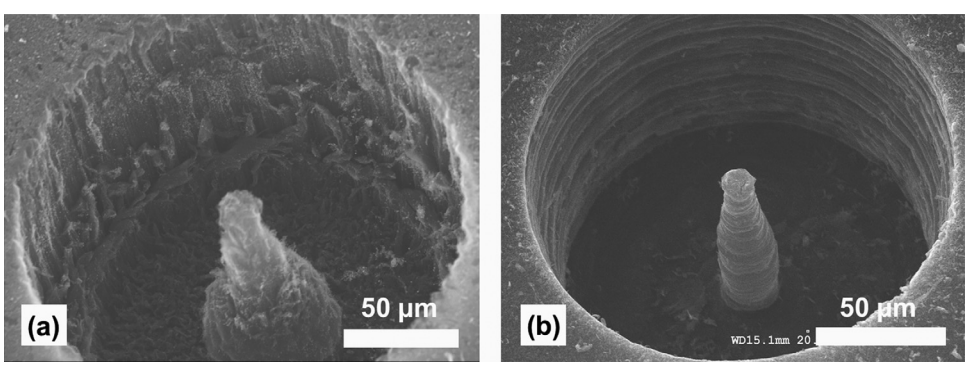


FIG. 6. SEM images of patterned high-aspect-ratio microstructures: (a) a cone shaped with normal polarity at 60 V and 10 pF by scanning a tapered electrode along a circular orbit with 90 $\mu$m diameter while feeding the electrode in the Z direction with 1-$\mu$m steps; (b) a cone shaped with reverse polarity at 10 V and 10 pF under the same scanning/feeding conditions as in (a). The height of both cones is 120 $\mu$m.

by patterning conical microstructuers with the conventional normal-polarity condition at 60 V as well as with the reverse-polarity condition at 10 V (both with 10 pF) using a tapered cyrindlical electrode. As can be seen from the results in Fig. 6, reverse $\mu$EDM achieved finer structures with higher aspect ratios and smoother surfaces, demonstrating its effectiveness with low discharge energies for high-aspect-ratio patterning in CNT forests. Since the discharge energy is equal to $CV^2/2$, where $C$ is the capacitance of the $R$-$C$ circuit (ignoring parasitics) and $V$ is the voltage, the above electrical conditions and results suggest that the discharge energy involved in the reverse-polarity case is 0.5 nJ, 36× smaller than the energy for the normal-polarity case (and ~80× smaller than the energy used for the high-aspect-ratio machining reported in Ref. 16), and that reverse-polarity $\mu$EDM enables proper CNT removal using such low discharge energies.

Energy-dispersive X-ray spectroscopy (EDX) of the CNT forest surfaces machined at 10 V and 10 pF [Fig. 7] indicated no detectable signals relevant to the electrode material (tungsten) with both the reverse and normal polarities, suggesting that the use of the reverse polarity involves almost zero consumption of the electrode and thus does not cause contamination of the processed forest surfaces with the electrode material. A high level of silicon detected in addition to carbon is most likely due to the presence of the substrate below the forest. These observations are also consistent with the previous results.[15] (Although the data shows a larger silicon peak for the normal-polarity case as seen in Fig. 7, we have not observed a similar behavior in other samples studied. Therefore, we believe this could be related to the nonuniformity in the initial thickness of the forest that has led to a difference in the forest thickness left after the removal, rather than an effect related to polarity.) Raman spectroscopy provided no evidence of significant $I_D/I_G$ ratio reduction,

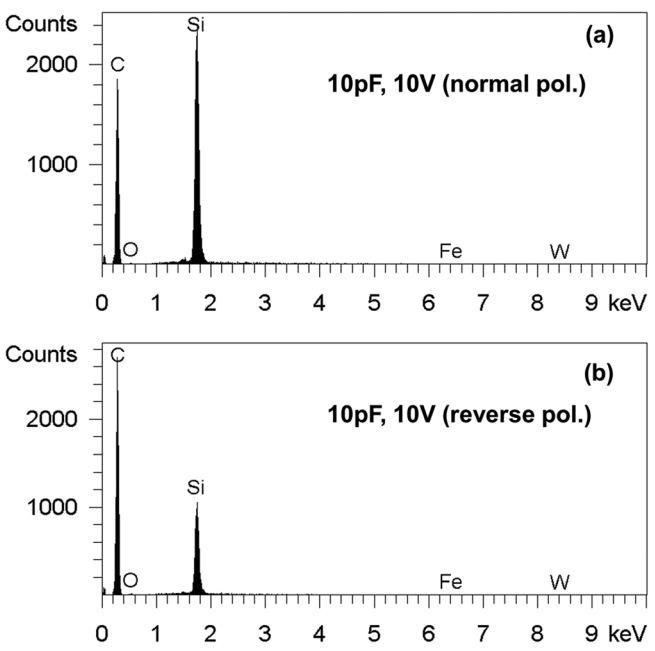


FIG. 7. EDX analysis results for the CNT-forest surfaces machined with (a) normal polarity and (b) reverse polarity.

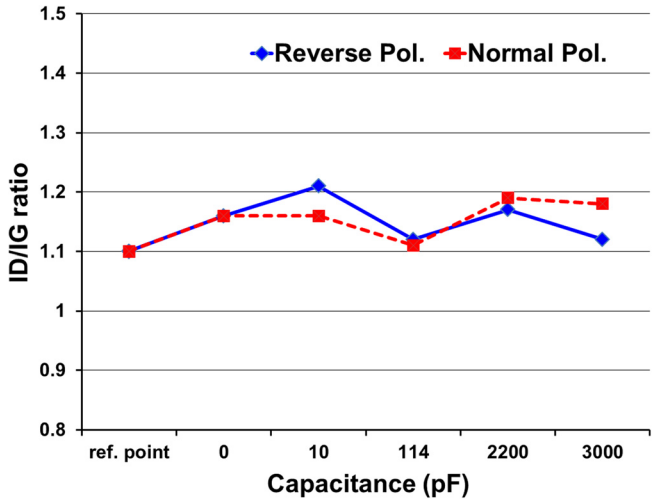


FIG. 8. (Color online) Raman ID/IG ratios for a forest sample machined at 30 V with different capacitor values.

i.e., increased defects in the CNTs processed with either polarity under different conditions [Fig. 8].

## IV. CONCLUSIONS

The effect of using reverse polarity in $\mu$EDM was investigated for micropatterning of pure CNT forests. It was found that the process with the reverse-polarity condition increased the discharge current, possibly because of the field-emission properties of CNTs that serve as the cathode in reverse $\mu$EDM. This concept was utilized to achieve $\mu$EDM of CNT forests at lower machining voltages or discharge energies compared to the previously reported conditions. The structures machined with reverse $\mu$EDM at low voltages were found to have higher precision and smoother and cleaner surfaces with almost no debris compared with those produced using conventional, normal-polarity processing. Reverse $\mu$EDM was also found to enable more stable and faster machining of the forests. Raman and EDX analyses revealed that reverse $\mu$EDM did not cause significant crystalline defects in the processed CNTs and contamination of the forest surfaces with the electrode element, respectively.

## ACKNOWLEDGMENTS

The authors thank Mohamed Sultan Mohamed Ali for his assistance in use of the $\mu$EDM system. We also thank Mehran Vahdani Moghaddam and Parham Yaghoobi for assistance with the nanotube growth process. This work was partially supported by the Natural Sciences and Engineering Research Council of Canada, the Canada Foundation for Innovation, and the British Columbia Knowledge Development Fund. K. Takahata is supported by the Canada Research Chairs program. A. Bsoul acknowledges financial support from the Jordan University of Science and Technology.

[1]M. M. J. Treacy, T. W. Ebbesen, and J. M. Gibson, Nature **381**, 678 (1996).
[2]J. P. Lu, Phys. Rev. Lett. **79**, 1297 (1997).
[3]K. Hsieh, T. Tsai, D. Wan, H. Chen, and N. Tai, ACS Nano **4**, 1327 (2010).

[4]Z. Yang, L. Ci, J. A. Bur, S. Lin, and P. M. Ajayan, Nano Lett. **8**, 446 (2008).
[5]N. Hamada, S. Sawada, and A. Oshiyama, Phys. Rev. Lett. **68**, 1579 (1992).
[6]Y. Hayamizu, T. Yamada, K. Mizuno, R. C. Davis, D. N. Futaba, M. Yumura, and K. Hata, Nat. Nanotechnol. **3**, 289 (2008).
[7]K. Kordás, G. Tóth, P. Moilanen, M. Kumpumäki, J. Vähäkangas, A. Uusimäki, R. Vajtai, and P. M. Ajayan, Appl. Phys. Lett. **90**, 123105 (2007).
[8]M. Chhowalla, C. Ducati, N. L. Rupesinghe, K. B. K. Teo, and G. A. J. Amaratunga, Appl. Phys. Lett. **79**, 2079 (2001).
[9]T. Y. Tsai, C. Y. Lee, N. H. Tai, and W. H. Tuan, Appl. Phys. Lett. **95**, 013107 (2009).
[10]S. Fan, M. G. Chapline, N. R. Franklin, T. W. Tombler, A. M. Cassell, and H. Dai, Science **283**, 512 (1999).
[11]Y. Jiang, P. Wang, and L. Lin, *24th IEEE International Conference Micro Electro Mechanical Systems, MEMS 2011, 23-27 January 2011* (Cancun, Mexico, 2011), pp. 396–399.
[12]J. Yang and D.-J. Liu, Carbon **45**, 2843 (2007).
[13]J. Flicker and J. Ready, J. Appl. Phys. **103**, 113110 (2008).
[14]L. Ge, S. Sethi, L. Ci, P. M. Ajayan, and A. Dhinojwala, Proc. Natl. Acad. Sci. **104**, 10792 (2007).
[15]W. Khalid, M. S. Mohamed Ali, M. Dahmardeh, Y. Choi, P. Yaghoobi, A. Nojeh, and K. Takahata, Diamond Relat. Mater. **19**, 1405 (2010).
[16]M. Dahmardeh, W. Khalid, M. S. Mohamed Ali, Y. Choi, P. Yaghoobi, A. Nojeh, and K. Takahata, *24th IEEE International Conference on Micro Electro Mechanical Systems (MEMS 2011)* (Cancun, Mexico, 2011), pp. 272–275.
[17]M. Dahmardeh, A. Nojeh, and K. Takahata, J. Appl. Phys. **109**, 093308 (2011).
[18]B. Liang, A. Ogino, and M. Nagatsu, J. Phys. D: Appl. Phys. **43**, 275202 (2010).
[19]M. P. Jahan, Y. S. Wong, and M. Rahman, J. Mater. Process. Technol. **209**, 1706 (2009).
[20]W. A. de Heer, A. Chatelain, and D. Ugarte, Science **270**, 1179 (1995).
[21]J.-M. Bonard, M. Croci, C. Klinke, R. Kurt, O. Noury, and N. Weiss, Carbon **40**, 1715 (2002).
[22]P. G. Collins and A. Zettl, Appl. Phys. Lett. **69**, 1969 (1996).
[23]Y. Saito, ed. *Carbon Nanotube and Related Field-Emitters—Fundamentals and Applications* (Wiley-VCH, 2010), p. 95.
[24]K. Sun, J. Y. Lee, B. Li, W. Liu, 1. C. Miao, Y. H. Xie, X. Wei, and T. P. Russell, J. Appl. Phys. **108**, 036102 (2010).
[25]H. C. Miller, IEEE Trans. Elec. Insul. **25**, 765 (1990).
[26]S. T. Purcell, P. Vincent, C. Journet, and V. T. Binh, Phys. Rev. Lett. **88**, 105502 (2002).